# Development of an enhanced heat transfer model of laminar pipe flow for pedagogical and research purposes

*Undergraduate Student Poster*

**Stone Simpson, Daniel Moreno**
*Missouri State University, Springfield, MO 65897*

## Abstract:

This research develops an advanced numerical model to study laminar pipe flow and its heat transfer characteristics, targeting both educational and research applications. Numerical methods are essential for solving complex fluid dynamics and heat transfer problems. Implemented in MATLAB, the model employs a 2-D finite difference approach within an axisymmetric cylindrical geometry to simulate temperature distributions and Nusselt numbers under various boundary conditions, including uniform heat flux (UHF), uniform wall temperature (UWT), and external convection. Verification against theoretical values shows the model's accuracy, closely matching the theoretical Nusselt numbers of 3.66 for uniform wall temperature and 4.36 for uniform heat flux. Simulations demonstrate how ambient temperature, convection coefficients, internal heat generation, and fluid viscosity influence heat transfer rates and efficiency. These findings are crucial for optimizing engineering designs such as heat exchangers and cooling systems. This study demonstrates the educational value and knowledge gained from numerical modeling, bridging theoretical knowledge and practical applications, and prepares students for advanced computational fluid dynamics (CFD) and related fields. This is done with very few starting fundamental equations. Adaptable to other programming languages, the model is versatile for various educational and research contexts. Future work will expand the model to include complex configurations like annular flow and concentric-pipe systems, enhancing its utility for academic and industrial applications. This research contributes to developing effective teaching tools in engineering education, fostering a deeper understanding of fluid dynamics and heat transfer through numerical modeling.

## Keywords:

Numerical modeling, heat transfer, laminar flow, pipe flow, undergraduate student poster

## Introduction:

As technology progresses, it is crucial for engineering students to develop competency in computational problem-solving skills to succeed independent of their career path [1, 2]. Much recent literature has focused on development of numerical modeling into engineering classes [3-5], citing its benefits in assisting complicated problems while prioritizing software approaches that use analytical techniques. Such numerical approaches to problem-solving can also be beneficial as they can be leveraged by existing knowledge that students have developed in their previous courses, including in mathematics [6]. However, students should still understand the underlying theory for programs to best interpret the results and understand limitations present in the model

[7]. Striking a balance between theory and application can be difficult [8-10], as there is only a limited amount of time that can be spent covering course material.

Several institutions have made it a point to implement advanced software techniques including computational fluid dynamics (CFD) into their curricula [11]. Some have even stressed the implications of going directly into CFD modeling for more advanced computational methods [12-14]. While learning the use of CFD can be invaluable in an undergraduate curriculum, it may not always be applicable to all undergraduates in preparation for their future careers. Furthermore, different workplaces and industries exhibit a myriad of different software techniques they use (including ANSYS, COMSOL, OpenFOAM, and Python) [15-18], so it may not be optimal to focus on just one technique for the selected software covered.

In this work, we develop a model for analyzing temperature distributions in pipe flow for a heat transfer course for mechanical engineers. The initial intent of the model was to introduce students to 2-D numerical modeling, a requirement for the courses, while also integrating the core analytical differential equation that is necessary to determine temperature regarding radial and axial positions [19]. The model acts as a pseudo-1-D transient model, assuming an axisymmetric cylindrical geometry and an initial condition for velocity and temperature distributions at the inlet of the pipe. The model is then advanced forward in the axial position, considering boundary conditions set at the inner walls of the pipe. As students have been introduced to 1-D transient variations in the course, this serves as a direct connection to that previous material. Presently, the model is developed in MATLAB, but provisions are made to adapt to other programming languages, such as Python.

The model's reliance on the core thermal energy equation for fluid transport enables it to be adapted to a wide set of fluid parameters, boundary conditions, and can consider different forms of internal heat generation, such as viscous dissipation. The only notable limitations to the model are that (1) constant fluid properties are assumed, and (2) the flow remains laminar, since the effects of turbulence from the equation are not considered and would serve to enhance the heat transfer via additional mixing in other directions.

This paper primarily serves as a basic outline of the model, its uses, and illustrates sample sets of temperature variations in the model. The radial and axial variations in temperature can both be used to determine the Nusselt number relating convective and conductive forms of heat transfer. As uniform heat flux (UHF) and uniform wall temperature (UWT) are commonly cited boundary conditions for Nu which can be developed without the need for experiments, these values will be confirmed first. Then, alternative cases such as employing external convective conditions (i.e. heating/cooling of the pipe), and the effects of internal heat generation on the Nusselt number will also be explored. Future modifications to the model will include annular flow with an internal boundary condition, useful in examining the performance of mapping temperature distribution in heat exchangers. While existing CFD software can serve as much more powerful means of illustrating all of the work that has been developed, here we demonstrate that nearly the same can be done using simpler tools building on and reinforcing existing concepts of the heat transfer fundamentals that have already been developed in the classroom.

## Theoretical Development:

The model developed is based on the heat equation for a cylindrical geometry, which is covered in the earlier stages of the heat transfer course (ME 3525 at Missouri S & T). The general heat equation for a constant property fluid undergoing laminar flow is given by:

$$\rho C_P \frac{\partial T}{\partial t} + \rho C_P u \cdot \nabla T = k\nabla^2 T + q'''_{gen} + \mu\Phi \quad (1)$$

where ρ is the density, $c_p$ is the specific heat capacity, u is the velocity vector, k is the thermal conductivity μ is the viscosity, $q_{gen}$''' represents any internal heat generation, and Φ is the viscous dissipation term, which is quite complicated [20]. It should be noted that when velocity terms are removed, this simplifies to the axial conduction equation for solids [21]. This equation, combined with appropriate boundary and initial conditions, allows us to simulate the temperature distribution within the pipe.

Although this model can have lots of different variable properties, some system constants were selected to investigate. The constants used for all simulation investigations are present in Table 1 below. Room temperature liquid water was used for the simulations, and its properties were assumed to remain constant with temperature during the experiments.

Table 1. Parameters used for numerical model.

| **Parameter** | **Symbol** | **Value** | **Units** | **Description** |
|---|---|---|---|---|
| Length | L | 50 | m | Length of the pipe |
| Radius | R | 0.01 | m | Radius of the pipe |
| Average Velocity | $U_{Avg}$ | 0.1 | m/s | Average velocity of the fluid |
| Density | ρ | 1000 | $kg/m^3$ | Density of water |
| Specific Heat | $c_p$ | 4200 | J/kg*K | Specific heat capacity of water |
| Thermal Conductivity | k | 0.6 | W/(m*K) | Thermal conductivity of water |
| Viscosity | μ | 0.001 | Pa*s | Dynamic viscosity of water |
| Radial Nodes | M | 50 | - | Number of discrete axial nodes |
| Axial Nodes | N | 50000 | | Number of discrete axial nodes |

Here, the fluid flow will be considered steady and hydrodynamically fully-developed, in order to maintain the focus on temperature variations. For laminar flow, this will yield a parabolic profile for the velocity distribution, with the maximum value occurring in the center of the pipe at a value of double the average velocity specified in Table 1.

$$u(r) = u_{max}\left(1 - \left(\frac{r}{R}\right)^2\right) \quad (2)$$

Neglecting variations in time as well as the effects of axial conduction, the energy equation in (1) can be simplified to:

$$\rho C_P u(r)\frac{\partial T}{\partial x} = k\left(\frac{1}{r}\frac{\partial}{\partial r}\left(r\frac{\partial T}{\partial r}\right)\right) + q'''_{gen} + \mu\left(\frac{\partial u}{\partial y}\right)^2 \quad (3)$$

The energy equation in (3) is then discretized into a grid of different nodes each representing radial and axial locations within the pipe (Figure 1). As all problems considered up to this point are axisymmetric, the setup is essentially a 2-D numerical model. Equation (3) can then be rearranged to isolate the axial temperature derivative, as this will be used as a pseudo time step to progress along the length of the pipe.

$$\frac{\partial T}{\partial x} = \frac{k}{\rho C_P u(r)}\left(\frac{\partial^2 T}{\partial r^2} + \frac{1}{r}\frac{\partial T}{\partial r}\right) + \frac{q'''}{\rho C_P u(r)} + \frac{\mu\Phi}{\rho C_P u(r)} \quad (4)$$

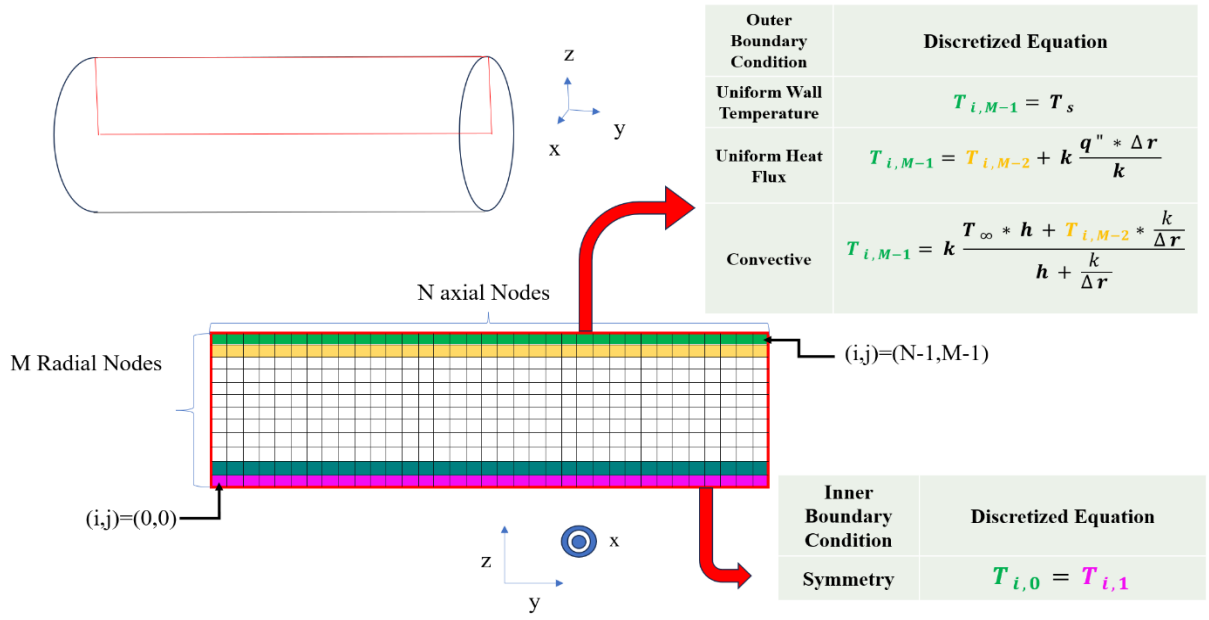


| Outer Boundary Condition | Discretized Equation |
|---|---|
| Uniform Wall Temperature | $T_{i,M-1} = T_s$ |
| Uniform Heat Flux | $T_{i,M-1} = T_{i,M-2} + k\frac{q'' * \Delta r}{k}$ |
| Convective | $T_{i,M-1} = k\frac{T_\infty * h + T_{i,M-2} * \frac{k}{\Delta r}}{h + \frac{k}{\Delta r}}$ |

| Inner Boundary Condition | Discretized Equation |
|---|---|
| Symmetry | $T_{i,0} = T_{i,1}$ |

Figure 1. Illustration of grid setup.

Under the constants taken from Table 1, a grid with N axial nodes and M radial nodes bound. N is bound to x=0 to x=L, and M is bound to y=0 to y=R Boundary conditions were applied to the top and bottom surfaces of the grid. On x=0 to x=L when M=0, the temperature of the N'th node is equal to the M=1 Nth node in the same N column. This exploits the axisymmetric properties of the system to reduce computational costs. The top M layer is under a separate set of boundary conditions. Three sets of boundary conditions are investigated here: UHF (Uniform heat flux), UWT (uniform wall temperature), and external convection. Table 2 summarizes how the boundary conditions are developed in the model.

Table 2. Summary of boundary conditions used in model.

| Inside Boundary Condition | Differential Form | Discretized Form | Theoretical Nusselt Number |
|---|---|---|---|
| Constant Temperature | $T(x,r=R_o)=T_s$ | $T_{i,M-1} = T_s$ | *3.66* |
| Constant Heat Flux | $k\frac{\partial T(x,r=R_o)}{\partial r} = q''$ | $k\frac{T_{i,M-1} - T_{i,M-2}}{\Delta r} = q''$ | *4.36* |
| Convective | $k\frac{\partial T(x,r=R_o)}{\partial r} = h(T(x,r=R_o)-T_\infty)$ | $k\frac{T_{i,M-1} - T_{i,M-2}}{\Delta r} = h(T_{i,M-1}-T_\infty)$ | - |

The scaling of M and N affects the amount of error acquired thought the course of the simulation. However, the values must be selected carefully to prevent stability errors (15) while optimizing computational time. As M scales linearly, N must grow at an exponential rate to reach stability within the system and produce a Nusselt number for the last N node. As both M and N increase, the calculated Nusselt number approaches the values in Table 2 for each boundary condition.

Here, a combination of a second order central difference and single order forward difference scheme is used to solve for the N middle nodes. This, combined with the first-order implementation of the boundary conditions are used to solve for the remaining nodes. This is continued axially down the pipe creating the temperature distribution. The use of the central difference solving method is something that when implemented decreases the difference between the known Nusselt numbers and the calculated Nusselt numbers. Figure 2 summarizes the procedure for performing the numerical calculation.

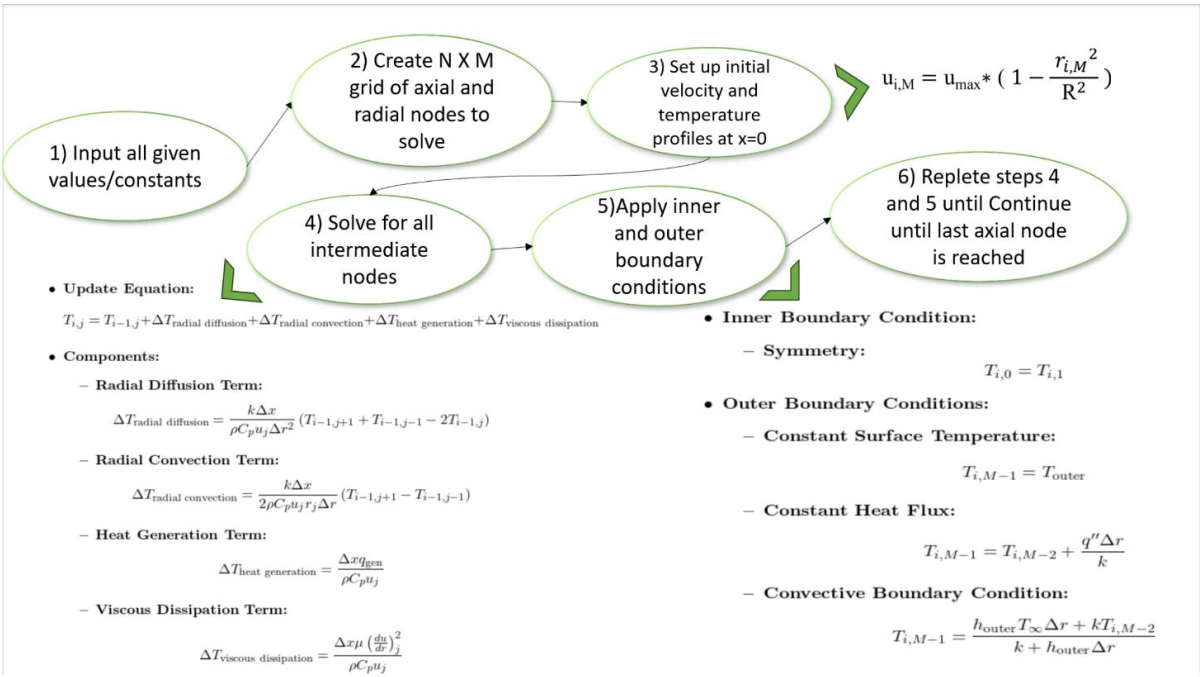

Figure 2. Summary of numerical model procedure

In the model, Nusselt number is taken only as a function of the axial position x of the pipe. Therefore, the average temperature along the length of the pipe must first be computed. This calculation is given by:

$$T_{avg} = \frac{\int T(r)u(r)dA}{\int u(r)dA} \quad (5)$$

where the integrals can be computed by simply using a set of Reimann sums for the number of radial positions M available. The Nusselt number can be computed from the equation:

$$Nu_D = \frac{hD}{k} \quad (6)$$

where in this equation only, h is an internal convection coefficient for the fluid, and is determined by solving:

$$-k\frac{\partial T(r=R)}{\partial r} = h\big(T(r=R) - T_{avg}\big) \quad (7)$$

where the temperature gradient $\frac{\partial T}{\partial r}$ in the conduction term is taken as an approximation between the two node values closest to the wall.

## Results & Discussion:

### Verification of established Nusselt numbers:

The first and most important step to verify the model is to compare the results it produces with known theoretical values. This is most effectively done by computing Nusselt numbers for the UHF and UWT conditions. In order to set up for this, temperature contours for all cases are provided first, to provide visual cues for how temperature varies in the pipe along both radial and axial position. From there, the average temperature along the axial position of the pipe can be better understood prior to plotting it explicitly on a linear graph, and subsequently the Nusselt number evaluated following the set of equations outlined previously.

The temperature contours for the UWT and UHF conditions were first investigated. The heat generation term in the equation was set to zero and the viscosity is kept at .001 Pa*s which accounts for a negligible amount of energy addition into the system. When wall temperature is kept constant (Figure 3A), the contour shows that the internal fluid temperatures approach that temperature along the pipe length, but the approach becomes more gradual as the distance between the lines grows larger. On the contrast, the UHF condition (Figure 3B) demonstrates a nearly linear temperature increase past the initial 5-10 meters for most of the fluid, as the gap between the lines stays nearly consistent. In both graphs, the constant temperature lines will always align parallel at the center of the pipe; this is in order to account for the necessary symmetry condition in which the radial temperature gradient must disappear.

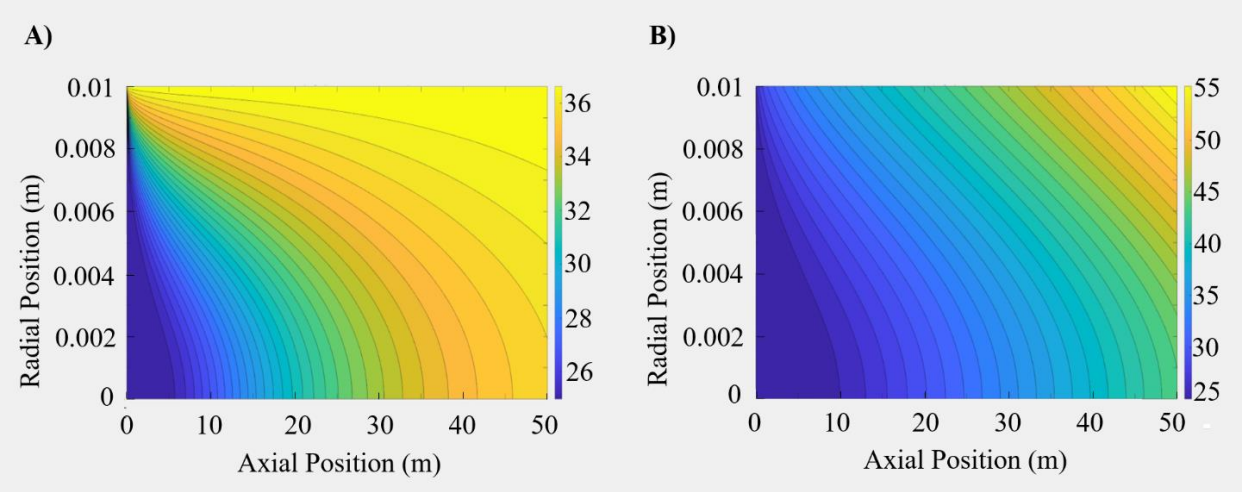


Figure 3. (A) Uniform wall temperature contour (50°C), (B) Uniform heat flux plot (1 kW/m$^2$).

The axial temperature gradients can be more clearly visualized when averaging the pipe temperature's radial position. Here, the trends align with what had been previously shown. For UWT, the average pipe temperature gradually approaches that of the set wall condition, while for UHF, the increase continues linearly (Figure 4A). As water would reach a phase change should its temperature exceed 100°C, here the model is limited in the maximum possible heat flux or length that could be used. For both conditions, the Nusselt number (Figure 4B) starts high but begins to approach a constant value as the flow thermally develops. The explanation for the high initial Nusselt number is that in both cases, the higher wall temperature accelerates the rate of convection between the rest of the fluid, while at the wall itself, temperature gradients are considerably smaller. Further downstream, the convective effects inside the pipe are less pronounced, and the steady-state values can be deduced. These are indeed the 3.66 for UWT and 4.36 for UHF, confirming that the model can effectively replicate the established theoretical values for laminar pipe flow.

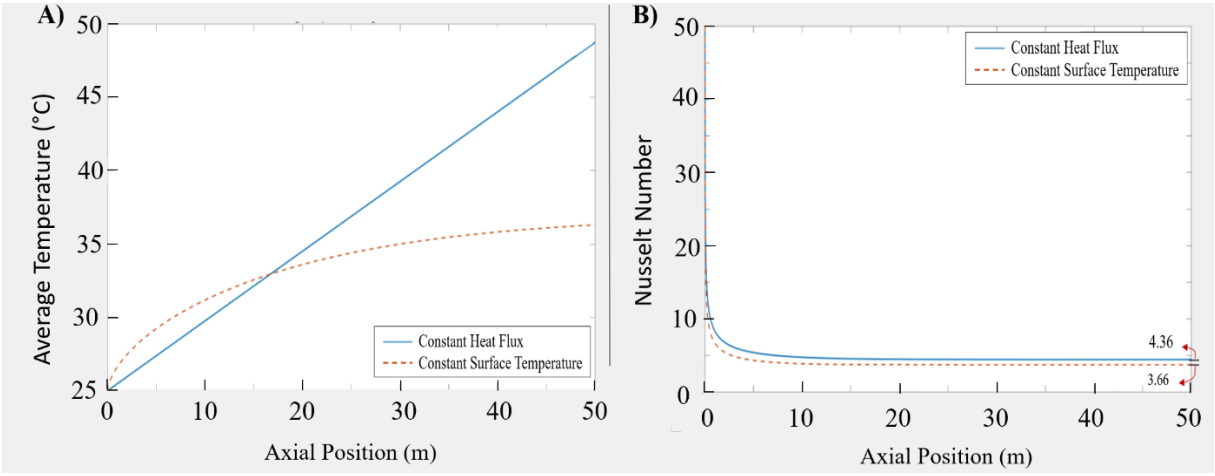


Figure 4. (A) UWT and UHF axial average temperature, (B) UWT and UHF axial Nusselt number.

## Nusselt number for external convection boundary condition:

With the theoretical values confirmed, the Nusselt number can then be evaluated for the one remaining condition: the external convective boundary condition. Here, the model can be set up in the same way, with the only difference that now an external convective coefficient and ambient temperature must be selected. Here, to simulate a realistic condition, we will consider a heated stream of water, initially at a uniform temperature of 80°C, which is exposed to an ambient temperature of 20°C with a convection coefficient of 5 $W/m^2*K$. This is an example best shown in the earlier stages of the Heat Transfer course when considering 1-D transient conduction through a wall. In that example, students generally understand that the outside will cool first since it is directly exposed to the ambient, and the insides will cool gradually afterward due to the natural tendency of heat to flow in the direction opposite temperature gradients according to Fourier's law. This is confirmed in Figure 5A and is visualized in the temperature contour. The center of the pipe is more capable of retaining its heat, but eventually will begin to cool as the outer layers of the fluid lose heat to the ambient. The average temperature along the pipe (Figure 5B) follows a similar predicted exponential trend as in the case with uniform wall temperature, only here the case is that the approached temperature is cooler rather than hotter. For the Nusselt number (Figure 5C), an interesting trend emerges: There appears to be a thermal development as a constant value is reached, but the constant value in this case is 4.24. Nusselt numbers for this configuration for laminar flow have not been as extensively reported, although this type of boundary condition is generally much more common in nature than either a UWT or UHF condition. This prompts a further investigation into the effect of whether the external convection coefficient or the outside temperature will significantly affect this Nusselt number.

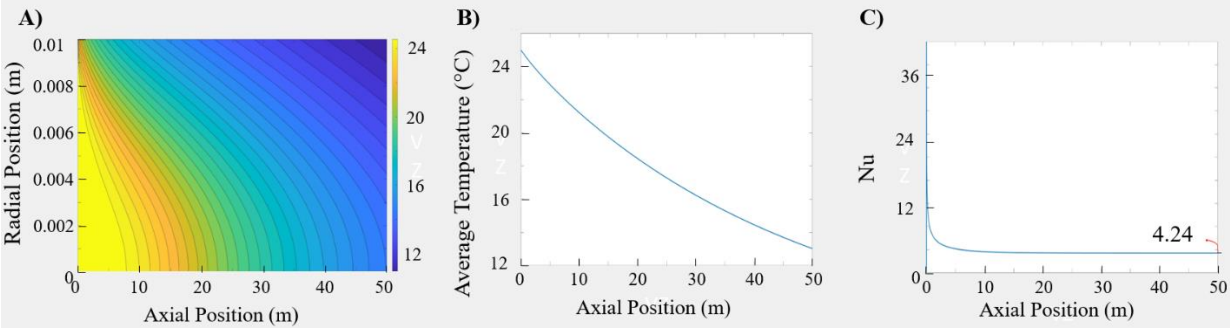


Figure 5. Convective boundary condition (5 W/m2*K, 20C ambient). (A) Temperature contour, (B) Average axial temperature °C, (C) Nusselt number.

The convective boundary condition, governed by the selection of the convection coefficient with the ambient temperature, and said ambient temperature, were plotted on a two-dimensional contour to demonstrate effects of the end-range (exit) temperature. Here, a range of convection coefficients and ambient temperature values are selected, with h ranging from 5 to 500 W/m2*K, and $T_\infty$ ranging from -10 to 50°C, to best simulate a range of outside conditions. The contour (Figure 6) shows that Nusselt number is more immediately affected by the external convection coefficient than by the outside temperature. The Nusselt number is maximized if the external convection coefficient is lower, despite what one might think about greater convection enhancing heat transfer. This is attributed to a lower radial heat transfer rate at the pipe wall when the convection coefficient

is lower, since heat cannot escape the pipe as quickly. Therefore, conduction effects will shrink, and a greater portion of the heat transfer will be due to the motion of the fluid instead. It should also be noted that the difference is notable but not extremely significant: Higher convection coefficients will only decrease Nusselt number from 4.78 to 4.24, or about 12%. It is interesting to note this range is still reasonably close to the previously studied boundary conditions, with convection coefficients of around 250 $W/m^2*K$ nearly equaling the Nu for the UHF boundary condition. While the results shown here may need to be more carefully investigated for other properties and conditions involving laminar flow, they can nonetheless serve as a good first approximation to laminar heat transfer pipe flow problems under this boundary condition.

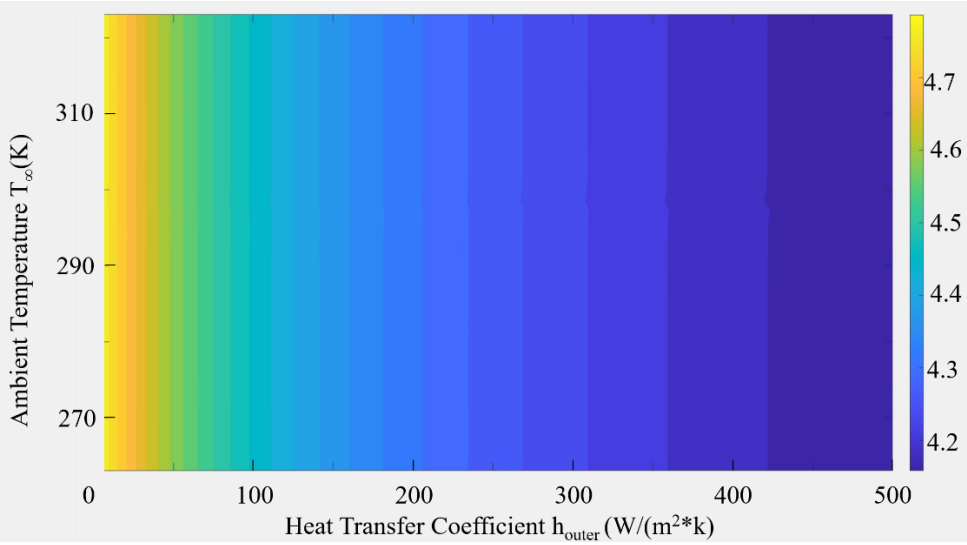


Figure 6. Ending Nusselt Number and its relation between $h_{outer}$ and $T_\infty$.

## Heat generation and viscous dissipation:

The effect of heat generation within the system have also been studied and investigated. Present in Figure 7 are graphs displaying the relationships the $q_{gen}'''$ term and its value have on the ending Nusselt number, average temperature, and ending temperature contour. These tests were run with a outer convection coefficient of 70 $W/m^2$ and a ambient temperature of 20°C.

Three different cases for heat generation are considered: 0 $W/m^3$, 50000 $W/m^3$, and 75000 $W/m^3$. Here, the pipe enters at 25°C and is exposed to an ambient at 20°C, so the case of zero heat generation will result in the fluid cooling, the intermediate heat generation rate maintain the same temperature, and the higher heat generation rate will raise the temperature.

When comparing temperature contours (Figure 7), the convective boundary condition plot resembles the temperature contour established in Figure 3A. If the heat flux is selected to maintain the inlet temperature, an interesting pattern emerges (Figure 7B): Initially, not enough heat is generated from the fluid, and the temperature distribution in the inner half of the pipe remains

mostly consistent at axial positions to about 5 m. After 10 m, the heating effect from the inside of the pipe is more clearly pronounced, and a clear gradient in the temperature is established through the pipe radially. In effect, this resembles a 1-D temperature distribution within a solid when uniform heat generation is considered. The value is maximum at the center, but this maximum is slowly approached and maintains a symmetry boundary condition, while the outside is coolest and rapidly loses heat to ambient. When the heat generation value is doubled, the horizontal temperature lines are no longer present, and the temperature increases further.

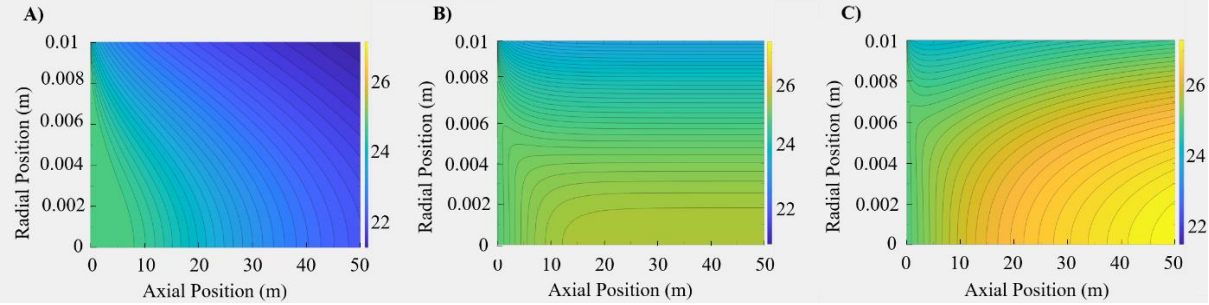


Figure 7. Temperature contours of convective boundary conditions. (A) No heat generation, (B) 50000 W/m$^3$, (C) 75000 W/m$^3$.

The axial temperature values (Figure 8A) follow the predicted trends for each heat generation case, but the Nusselt number (Figure 8B) yields a more increased result: A higher heat generation rate will enhance heat transfer, but the enhancement does not appear to be linear. The steady-state values for 0, 50000, and 75000 W/m$^3$ are 4.41, 6.19, and 6.51 respectively. Here, the heat transfer rates begin to reach values beyond typically expected for laminar flow. If the heat generation rate is raised further, it is possible that an asymptote value for the Nusselt number could be reached.

Looking at the theoretical relations (Eq. 1), and the development for the UHF and UWT conditions, a relation between heat generation rate and Nusselt number could possibly be developed under these two boundary conditions, but the value would likely be property/geometry dependent as these terms would not disappear in the derivation.

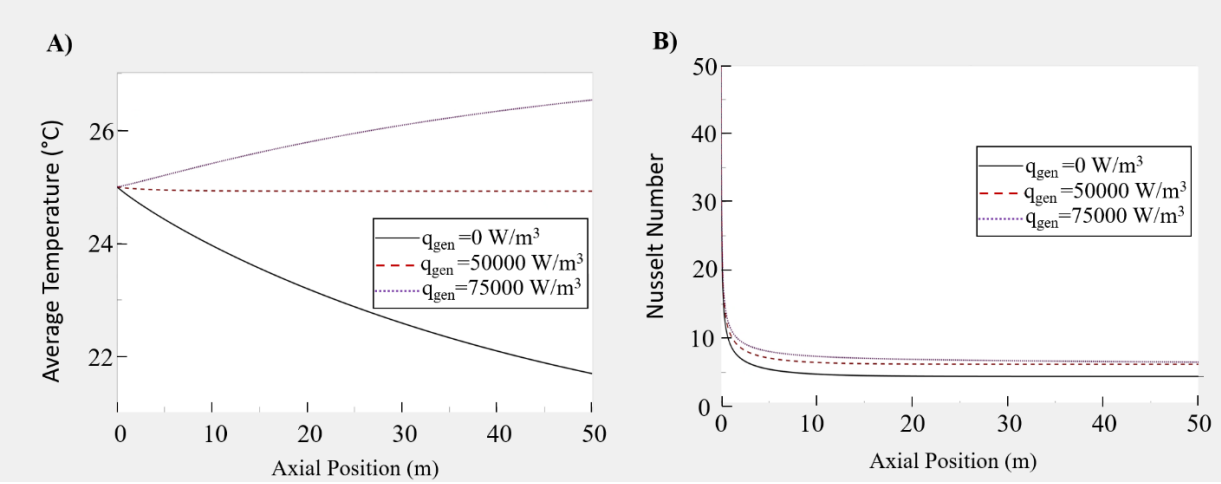


Figure 8. (A) Heat generation axial average temperature, (B) Heat generation axial Nusselt number.

For viscous dissipation, three different cases are considered: 0.001 Pa*s, 25 Pa*s, and 50 Pa*s. The temperature contours (Figure 9) reveal the gradual increase in temperature when viscosity in the fluid is increased; this is generally the "lost" energy for any type of fluid flow along the pipe. It should be noted that this temperature contour is a different shape than they are shown for arbitrary heat generation; here, the rise in temperature due to viscosity is proportional to the square of the velocity gradient (Eq. 1). Therefore, heating would occur more directly closer to the wall than to the center, although heat generated at the wall by friction is also lost to convection in this scenario. The generated heat then mostly accumulates at the center.

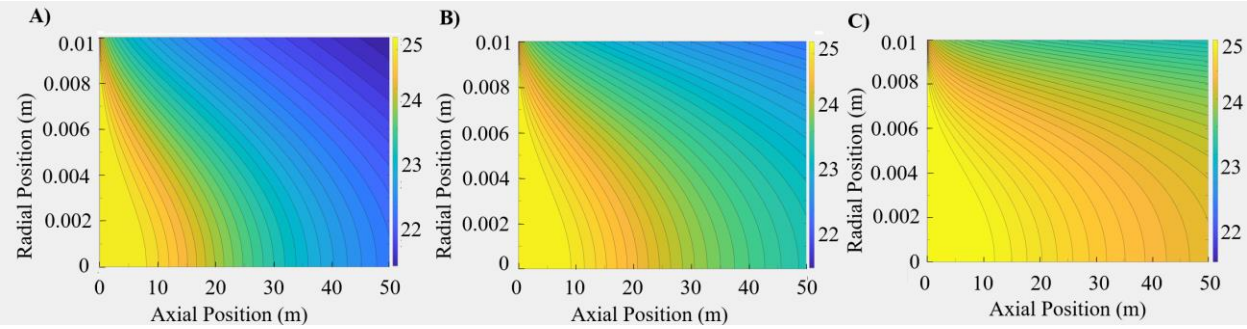


Figure 9. Temperature contours of convective boundary conditions. (A) 0.001 Pa*s, (B) 25 Pa*s, (C) 50 Pa*s.

In the examples considered here, the viscosity is not high enough to compensate for external convection losses, so higher viscosities essentially equate to a lower heat loss (Figure 10A). As was done with generation, viscosity could be increased further to determine the minimum value necessary to offset convection losses, and a plot similar to the one shown in Figure 8A could be obtained.

For the Nusselt number, the values once again converge, and the higher viscosity enhances the heat transfer quite substantially (Figure 10B). At 25 Pa*s, the Nusselt number reaches 6.3, and at 50 Pa*s, the value nearly doubles from the base case with negligible dissipation to nearly 8.2. Here, the effect is similar to that seen previously for heat generation, where a higher viscosity creates shallower temperature gradients. At the wall, this decreasing rate of conductive heat transfer and enhancing the amount of heat transfer must be caused by advection. The result is somewhat counter to traditional heat transfer logic, as higher viscosities would slow down the rate of heat transfer, but for laminar flow, convection coefficient is not directly affected by dimensionless numbers. Since the viscosity in these examples is higher, velocity could be altered to examine changes in the trends while maintaining laminar flow. Like with heat generation, this effect could be examined theoretically for the UWT and UHF conditions, to determine if some dependence or convergence to a steady-state Nusselt number with viscosity is reached.

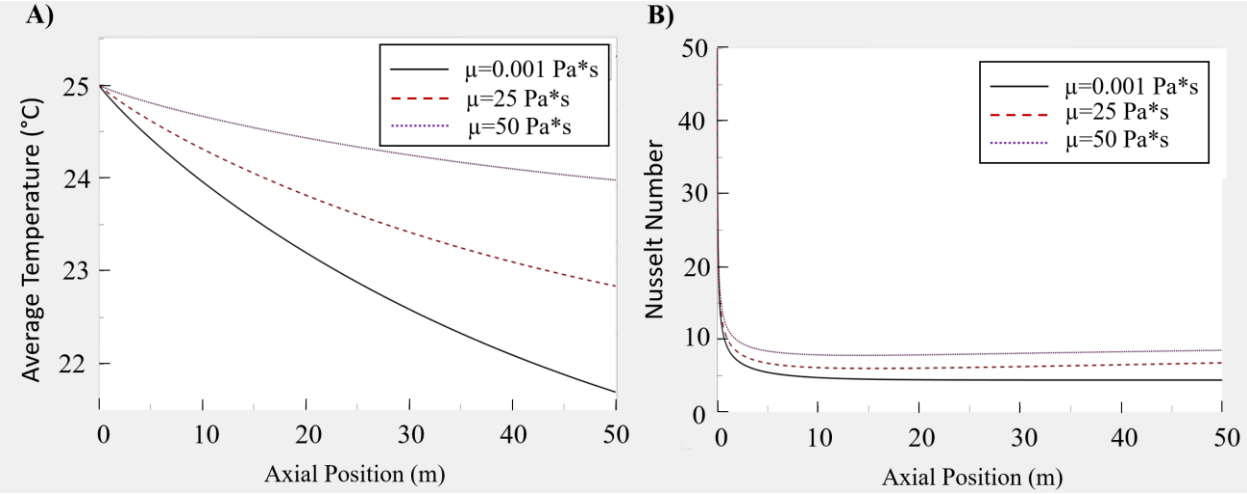


Figure 10. (A) Viscous dissipation axial average temperature, (B) Viscous dissipation axial Nusselt number.

## Conclusion:

This paper discusses in detail the development a 2-D asymmetric numerical model for laminar pipe flow. The setup serves to balance introducing students to the benefits and wide range of options offered by the numerical modeling, while also maintaining core principles of heat transfer and the energy equation that have been previously developed. The model produces temperature contours for both radial and axial positions, average temperature along the axial length, and Nusselt number along the axial length. The calculation of Nusselt number is used to verify that the model produces the familiar values for uniform wall temperature (UWT) and uniform heat flux (UHF) conditions, confirming the accuracy of the model. From there, the more realistic external convection boundary condition is applied, and it shown that the Nusselt number falls within a close range relative to the UWT/UHF conditions, but is actually enhanced when the convection coefficient is lower, which can be useful for first estimates of the value under this condition. Finally, as they are included in the generalized form of the energy equation, heat generation and viscous dissipation are each explored under three different cases. The cases highlight how increases in temperature occur primarily in the center of the fluid, and also show that increases in both values will enhance the Nusselt number for heat transfer, in some cases exceeding double the values for the case with negligible heat generation.

In summary, the numerical pipe flow model has been developed for a set of simple cases to better bridge the gap between computational modeling and familiar theoretical principles, which can be circumvented if only graphical software such as computational fluid dynamics is used, with minimal condition to the underlying equation. Here, it is shown that with only the energy equation and a set of boundary conditions, several key heat transfer characteristics can be examined, and a range of customizable parameters and conditions can be explored. This initial exposure can serve as a benefit to students who will go into advanced CFD modeling in more detail, as well as those who may continue to do similar numerical modeling or programming. In the future, the model will be expanded to consider configurations more useful in research or in industry, such as annular flow with an internal boundary condition or double-pipe flow for analysis of temperature distribution in a heat exchanger.

## Bibliography:


[1] J. Swart, "Theory versus practical in a curriculum for engineering students—A case study," in *AFRICON 2009*, 2009: IEEE, pp. 1-4.

[2] P. C. Wankat and F. S. Oreovicz, *Teaching engineering*. Purdue University Press, 2015.

[3] X. Le, R. L. Roberts, and A. W. Duva, "Teaching Finite Element Analysis for mechanical undergraduate students," in *2019 ASEE Annual Conference & Exposition*, 2019.

[4] A. Callejo and J. Garcí´ a de Jalo´ n, "Teaching undergraduate numerical methods through a practical multibody dynamics project," in *International Design Engineering Technical Conferences and Computers and Information in Engineering Conference*, 2011, vol. 54815, pp. 657-665.

[5] G. Zhu, L. Li, M. Xue, and T. Liu, "An effective educational tool for straightforward learning of numerical modeling in engineering electromagnetics," *Computer Applications in Engineering Education,* vol. 29, no. 6, pp. 1554-1566, 2021.

[6] J. Hu, L. Zhang, and X. Xiong, "Teaching computational fluid dynamics (CFD) to Design Engineers," in *2008 Annual Conference & Exposition*, 2008, pp. 13.1151. 1-13.1151. 11.

[7] E. Tempelman and A. Pilot, "Strengthening the link between theory and practice in teaching design engineering: an empirical study on a new approach," *International journal of technology and design education,* vol. 21, pp. 261-275, 2011.

[8] M. Andriychuk, *Numerical Simulation: From Theory to Industry*. BoD–Books on Demand, 2012.

[9] J. Červeňová, "OPTIMAL BALANCE OF ANALYTICAL AND NUMERICAL METHODS IN TEACHING OF ELECTROMAGNETISM," *DISTANCE LEARNING, SIMULATION AND COMMUNICATION 2013,* p. 27, 2013.

[10] A. J. Hughes and C. Merrill, "Solving Concurrent and Nonconcurrent Coplanar Force Systems: Balancing Theory and Practice in the Technology and Engineering Education Classroom," *Technology and Engineering Teacher,* vol. 80, no. 1, p. 16, 2020.

[11] W. Mokhtar, "Project-based learning (PBL): an effective tool to teach an undergraduate CFD course," 2010.

[12] J. D. Eldredge *et al.*, "A best practices guide to CFD education in the undergraduate curriculum," *International Journal of Aerodynamics,* vol. 4, no. 3-4, pp. 200-236, 2014.

[13] A. Fedyushkin and A. Puntus, "Revisiting the need to combine educational and scientific-research processes in teaching CFD modelling to students," in *Journal of Physics: Conference Series*, 2021, vol. 1809, no. 1: IOP Publishing, p. 012006.

[14] M. Rodríguez-Martín, P. Rodríguez-Gonzálvez, A. Sánchez-Patrocinio, and J. R. Sánchez, "Short CFD simulation activities in the context of fluid-mechanical learning in a multidisciplinary student body," *Applied Sciences,* vol. 9, no. 22, p. 4809, 2019.

[15] H. J. Kwon, "Use of comsol simulation for undergraduate fluid dynamics course," 2013.

[16] S. Verma, Z. Mansouri, and R. P. Selvam, "Incorporating two weeks open source software lab module in CFD and fluids courses," in *2021 ASEE midwest section conference*, 2021.

[17] M. N. SARIMURAT, "Integrating Theory and Practice: A CFD Education Approach," in *2024 ASEE Annual Conference & Exposition*, 2024.

[18] X. Li and S. C. Cheung, "A learning-centred computational fluid dynamics course for undergraduate engineering students," *International Journal of Mechanical Engineering Education,* p. 03064190231224334, 2024.

[19] T. L. Bergman, *Fundamentals of heat and mass transfer*. John Wiley & Sons, 2011.

[20] S. M. Ghiaasiaan, *Convective heat and mass transfer*. CRC Press, 2018.

[21] D. W. Hahn and M. N. Özisik, *Heat conduction*. John Wiley & Sons, 2012.

## Biography:

### Stone Simpson

Stone is a senior completing his Mechanical Engineering degree, driven by a passion for helping and providing for the community. Whether selling shoes or working on sewer maintenance, ensuring the people he serves are well informed and taken care of is his top priority. Beyond his studies, he leads projects with local cities to build websites in support of the EPA's Lead Service Inventory Project. On a never ending quest to learn the intricacies that lie in the world we live in, Stone dreams of advancing sustainable energy through algae research, envisioning a future where the world embraces this green resource.

### Daniel Moreno

Dr. Daniel Moreno is an Assistant Professor of Mechanical Engineering at Missouri State University's Cooperative Engineering Program, with a joint appointment in the PAMS (Physics, Astronomy, Materials Science) department and a courtesy appointment at Missouri University of Science & Technology. He received his Bachelor's degree in Mechanical Engineering at the Cooper Union for the Advancement of Science and Art in New York City. He received his Master's and Ph.D. at Georgia Institute of Technology, also in Mechanical Engineering. Dr. Moreno's teaching expertise is in the thermal sciences. At Georgia Tech, Dr. Moreno served as President for the institution's chapter for the American Society for Engineering Education. He presently teaches courses in thermal science in the Cooperative Engineering Program, where he hopes to incorporate relevant technical examples and ideas from his research into his teaching. His research integrates thermodynamics concepts in ME with the multi-disciplinary field of electrochemistry to promote renewable energy technologies.